Joint Pathology Center
Veterinary Pathology Services

WEDNESDAY SLIDE CONFERENCE 2012-2013

Conference 22

17 March 2013

CASE I: 48081 (JPC 4019425).

Signalment: 7-year-old, female spayed, domestic shorthair cat (*Felis catus*).

History: The cat had a history of acute onset of seizures with concurrent circling to right and a left menace deficit. Based on the MRI characteristics of rim enhancement and large amounts of perilesional edema, right thalamic abscess, neoplasia and granuloma were the top differential diagnoses. There was initially a good response to antibiotics and phenobarbital, and the cat was lost to follow-up for several months. The cat represented 14 months later, and demonstrated no response to repeat steroids, therefore, the owner elected euthanasia. An MRI was obtained prior to euthanasia revealing a large, right thalamic mass.

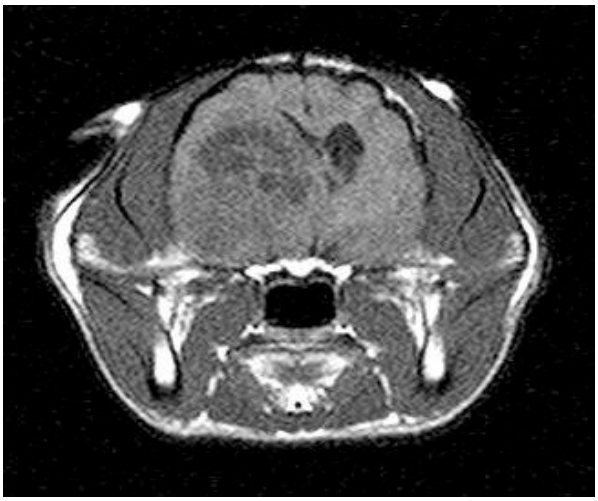

1-1. MRI of cerebrum at level of thalamus, cat: An MRI was obtained prior to euthanasia revealing a large, right thalamic mass. (Photo courtesy of the Department of Pathology, Animal Medical Center, 510 East 62nd St. New York, NY 10065. http:// www.amcny.org/)

1-2. Cerebrum, cat: At necropsy, there was asymmetric enlargement of the right cerebrum. (Photo courtesy of the Department of Pathology, Animal Medical Center, 510 East 62nd St. New York, NY 10065. http:// www.amcny.org/)

1-3. Cerebrum at level of thalamus, cat: Upon sectioning of the fixed brain, there is a 2 cm diameter, large, firm, tan to light yellow, gelatinous, cystic mass extending from the right cerebrum to the midbrain, expanding the pyriform lobe and compressing the right lateral and third ventricles and causing a midline shift. (Photo courtesy of the Department of Pathology, Animal Medical Center, 510 East 62nd St. New York, NY 10065. http:// www.amcny.org/)

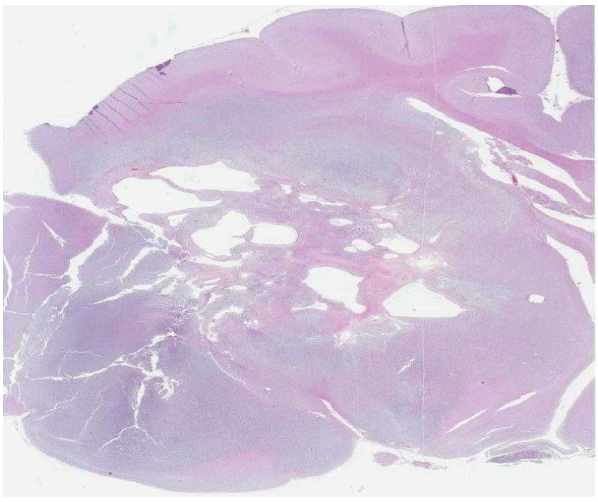

1-4. Cerebrum at level of thalamus, cat: Subgross image of tissue corresponding to Figure #3. (Photo courtesy of the Department of Pathology, Animal Medical Center, 510 East 62nd St. New York, NY 10065. http:// www.amcny.org/) (HE 0.63X)

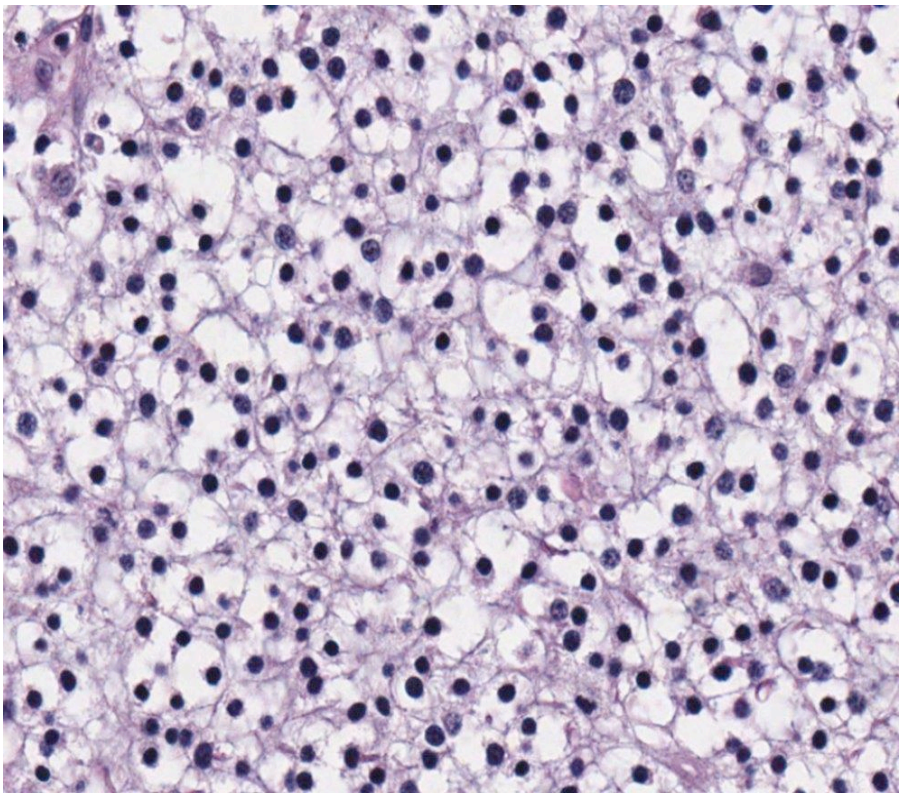

1-5. Cerebrum at level of thalamus, cat: Neoplastic cells form a characteristic "honeycomb" or "chicken-wire" arrangement, considered the result of artifactual retraction of cytoplasm. (Photo courtesy of the Department of Pathology, Animal Medical Center, 510 East 62nd St. New York, NY 10065. http:// www.amcny.org/) (HE 400X)

Gross Pathology: External examination of the brain from the dorsal and ventral aspects reveals asymmetric enlargement of the right cerebrum, involving the right pyriform lobe. Upon sectioning of the fixed brain, there is a 2 cm diameter, large, firm, tan to light yellow, gelatinous, cystic mass extending from the right cerebrum to the midbrain. The mass compresses the right lateral and third ventricles, causing a midline shift, with marked expansion of the pyriform lobe and obliteration of basal nuclei.

Laboratory Results: Cytology of the mass did not reveal any inflammatory cells.

Histopathologic Description: A section of the brain including the cerebral cortex and thalamus is examined at the level of the body and crura of fornix, basal nuclei, third ventricle and pituitary gland (not all slides contain pituitary gland). Within the thalamus, white matter of the

pyriform lobe and cerebral cortex of the temporal lobe, extending to involve the grey matter, there is a poorly demarcated, infiltrative, densely cellular neoplasm, consisting of round to polygonal cells forming sheets and cords amongst an eosinophilic fibrovascular to amphophilic myxomatous stroma. Neoplastic cells are mildly pleomorphic, with variably distinct cell borders, clear (perinuclear halo) to lightly stained vacuolated eosinophilic cytoplasm, and round, central nuclei. Nuclei are typically hyperchromatic, with indistinct chromatin and nucleoli. Mild anisokaryosis is observed, up to two fold. There are zero mitoses in ten high power fields. In some regions of the neoplasm, cell borders are prominent ("fried egg" or "honeycomb" pattern). Multifocally, vessels are conspicuous, characterized by prominent endothelial hypertrophy and proliferation (glomeruloid vessels). Clear, cystic spaces are dispersed throughout the center of the neoplasm, and a focus of hemorrhage is present in some slides. Within these regions, the white matter parenchyma is rarefied (edema), containing swollen axons (spheroids) and glial cells, including Gitter cells and gemistocytic astrocytes. Remnant neurons from the infiltrated neuroparenchyma and reactive glial cells are scattered throughout the neoplastic populations. In the section of pituitary gland, there is mild acidophil hyperplasia. Mild endothelial hypertrophy is present in the small vessels of the adjacent and contralateral cerebral cortex.

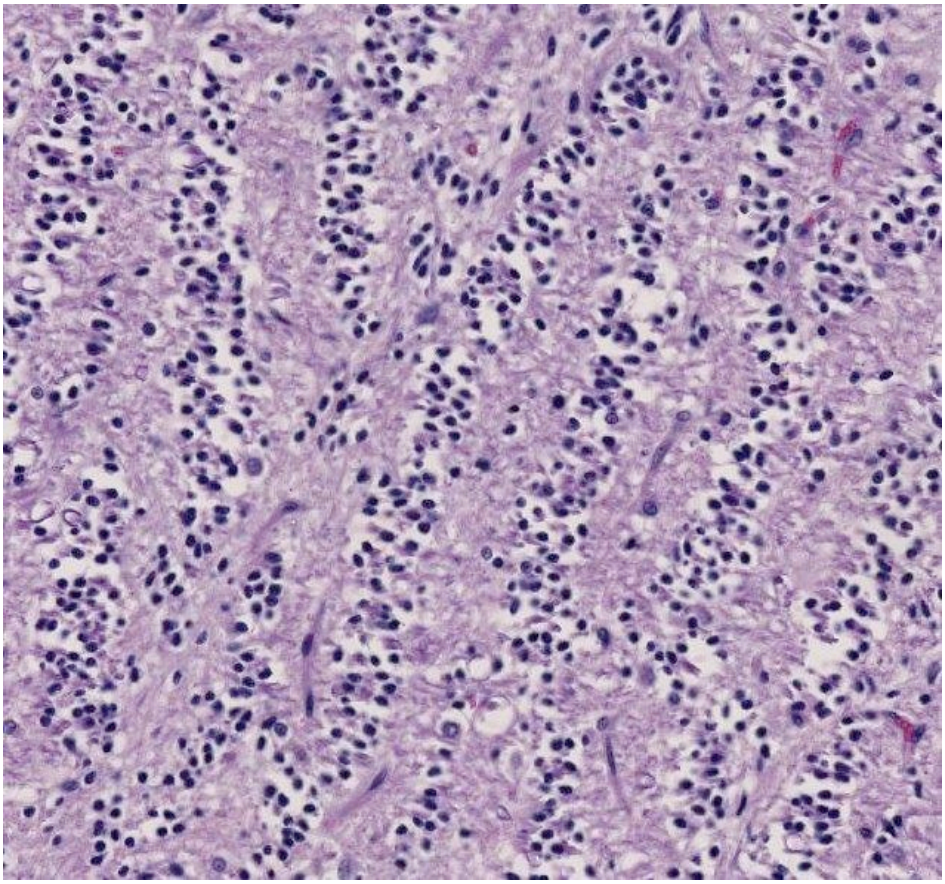

1-6. Cerebrum at level of thalamus, cat: In some areas of the neoplasm, nuclei are arrayed in characteristic "tiger striping" formations. (HE 400X)

Contributor's Morphologic Diagnosis: Brain (thalamus): Oligodendroglioma with intralesional and peripheral edema and gliosis.
Pituitary gland: Mild acidophil hyperplasia.

Contributor's Comment: Oligodendroglioma is a primary central nervous system neoplasm composed of oligodendrocytes, the myelin producing cells of the central nervous system (CNS). In cats, glial tumors are reported to be the fourth most common CNS neoplasm, preceded by meningioma, lymphoma and, in one study, pituitary neoplasms.[5,6] In a retrospective study of 160 cases of feline intracranial neoplasia, six oligodendrogliomas were reported, the median age for which was 9.3 years. Seizures were the most common clinical sign, along with altered consciousness, aggression, circling and ataxia in 2 cats.[6] A study analyzing tumor types and seizure patterns in 61 cats found that generalized seizures (vs partial seizures) were most common in cats with intracranial neoplasia. In that study, the highest incidence of seizures occurred with astrocytomas (33%), with a high overall incidence of seizures with all glial cell tumors (26.7%).[5]

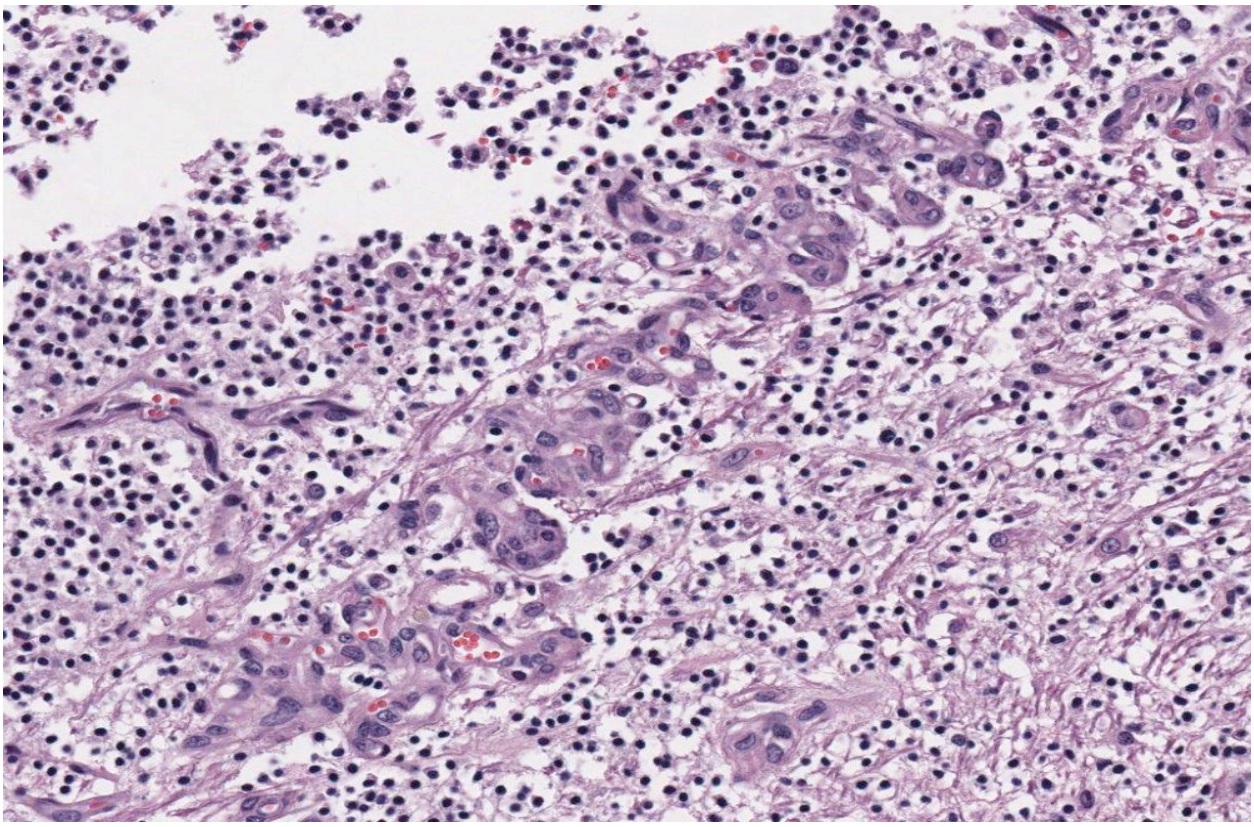

1-7. Cerebrum at level of thalamus, cat: Multifocally, vessels are conspicuous, characterized by prominent endothelial hypertrophy and proliferation (a.k.a "glomeruloid vessels"). (Photo courtesy of the Department of Pathology, Animal Medical Center, 510 East 62nd St. New York, NY 10065. http://www.amcny.org/) (HE 400X)

Oligodendrogliomas can occur in all areas of the white matter of the cerebrum, brainstem, and interventricular septum.[3,4,7] Feline oligodendrogliomas in the aforementioned larger case series were most commonly found in the temporal lobes, and all were located in the ventral portion of the brain, consistent with previous reports of this tumor in the deeper structures of the cerebral hemisphere.[5] In dogs, this tumor is more common in brachycephalic breeds.[3,4,6,7]

Macroscopic features of oligodendrogliomas range from soft and gelatinous to firm and they are frequently grey to pink-red, varying from well demarcated to poorly demarcated.[3,4,7] Neoplastic oligodendrocytes are typically uniform in cellular and nuclear size and shape, with rare mitoses. Characteristic features of this neoplasm include the clear to lightly stained cytoplasm (perinuclear halo) and a distinct cell membrane.[3,4,7] Autolysis is thought to lend to the "fried egg" or "honeycomb" appearance of the neoplastic cells.[1,3] Mucinous cystic degeneration, edema, cavitation and rarely mineralization can occur, and necrosis is rare. Prominent branching capillary proliferation forms a "chicken wire" vascular pattern.[3,4] At the margins of the tumor, neoplastic cells may be arranged in chains (as in this case), reminiscent of interfascicular oligodendrocytes.[3,4,7] Perivascular cuffing and satellitosis of neurons with neoplastic cells may occur in infiltrated grey matter.[4] Anaplastic oligodendrogliomas are characterized by nuclear pleomorphism, high cellularity, a high mitotic index, prominent vascularization, intratumoral necrosis and rarely, calcification.[1,4,7] The initial MRI findings of rim enhancement and perilesional edema could not differentiate neoplasia from inflammatory conditions including abscess and granuloma. A report detailing clinical and pathologic features of oligodendrogliomas in two cats found heterogenous contrast enhancement and hyperintensity of proton weighted (PW) and T2 weighted images and either iso or hypointensity on T1 weighted images in both cases.[1] Post contrast ring enhancement has been reported with CT scans of canine oligodendrogliomas.[1]

Some human oligodendrogliomas express S-100 protein and the Leu-7 marker, but this expression

pattern is not specific for oligodendrogliomas.[3] Immunoreactivity for GFAP may indicate the presence of early transitional glial cell forms.[3] Normal oligodendrocytes do not express GFAP, but immunoreactivity for GFAP can be demonstrated in up to 50% of human oligodendrogliomas, which may be due to reactive gemistocytic astrocytes.[1] A case series of two cats with oligodendrogliomas identified minigemistocytic astrocytes or gliofibrillary oligodendrocytes in one cat. These cells may represent a transitional form between neoplastic oligodendrocytes and astrocytes and appear identical to oligodendroglioma cells, but have a thin perinuclear rim of GFAP positive cytoplasmic staining.[1] GFAP immunohistochemistry was not performed in this case. Detection of smooth muscle actin expression in the glomeruloid vascular proliferation is a distinctive feature of anaplastic oligodendrogliomas of dogs.[1]

JPC Diagnosis: Brain, cerebrum at level of midbrain: Oligodendroglioma.

Conference Comment: The contributor's adept summary includes a brief discussion of patterns of immunohistochemical expression in oligodendrogliomas. Recently, Ide et al. explored several markers to identify characteristic immunohistochemical profiles for each of the eight types of canine neuroepithelial tumors (i.e. astrocytic tumors, oligodendroglial tumors, other gliomas, ependymal tumors, choroid plexus tumors, neuronal and mixed neuronal–glial tumors, embryonal tumors, and pineal parenchymal tumors).[2] They found that in oligodendrogliomas, the majority of cells were positive for doublecortin (DCX) but negative for glial fibrillary acidic protein (GFAP). Furthermore, benign oligodendrogliomas contained few nestin-positive cells compared to anaplastic oligodendrogliomas, which contained many nestin-positive cells. Two anaplastic oligodendrogliomas displayed positivity for Beta III tubulin. All cases of oligodendrogliomas were negative for neurofilament (NF), cytokeratin AE1/AE3, or cytokeratin 18. DCX plays a major role in neuroblast migration during cerebral cortex development. GFAP is an intermediate filament protein of mature astrocytes; nestin is an intermediate filament protein of immature astrocytes; NF is a marker for mature neurons; beta III tubulin is used to identify early neuronal differentiation; cytokeratin AE1/AE3 is used to identify many high- and low-molecular weight cytokeratins; and cytokeratin 18 is a simple epithelial cytokeratin.[2] As for expression of proliferation/ apoptosis markers in oligodendrogliomas, the following results were found: Generally, the percentage of Ki-67-positive cells were low, with the exception of two cases; p53 expression by more than 10% of tumor cells was observed in one case; there were higher numbers of Bcl-2 positive tumor cells in comparison to Bcl-xL-positive cells, and no cells showed positivity for epidermal growth factor receptor (EGFR), c-erbB2 (aka HER-2 or neu), phosphoextracellular signal-regulated kinase 1/2 pERK1/2, phospho-Akt (pAkt), or cleaved caspase 3.[2]

Contributing Institution: Animal Medical Center
510 East 62nd St.
New York, NY 10065
www.amcny.org/

References:

1. Dickinson PJ, Keel MK, Higgins RJ, Koblik PD, Lecouteur RA, Naydan DK, et al. Clinical and pathologic features of oligodendrogliomas in two cats. *Vet Pathol*. 2000;37:160-167.
2. Ide, Uchida K, Kikuta F, Suzuki K, Nakayama H. Immunohistochemical Characterization of Canine Neuroepithelial Tumors. *Vet Pathol*. 2010;47(4)741-750.
3. Koestner A, Bilzer T, Fatzer R, Schulman FY, Summers BA, Van Winkle TJ. Oligodendroglioma. In: *Histological Classification of Tumors of the Nervous System of Domestic Animals*. 2nd series. Vol. V. Washington, DC: Armed Forces Institute of Pathology; 1999:19-20.
4. Summers BA, Cummings JF, DeLahunta A. Oligodendroglial tumors. In: *Veterinary Neuropathology*. St. Louis, MO: Mosby-Year Book Inc; 1995:370-373.
5. Tomek A, Cizinauskas S, Doherr M, Gandini G, Jaggy A. Intracranial neoplasia in 61 cats: localisation, tumour types and seizure patterns. *J Feline Med Surg*. 2006;8(4):243-53.
6. Troxel MT, Vite CH, Van Winkle TJ, Newton AL, Tiches D, Dayrell-Hart B, et al. Feline intracranial neoplasia: retrospective review of 160 cases (1985-2001). *J Vet Intern Med*. 2003;17(6): 850-9.

7. Zachary JF. Nervous system. In: McGavin MD, Zachary JF, eds. *Pathologic Basis of Veterinary Disease*. 4th ed., St Louis, MO: Mosby Elsevier; 2007:951.

CASE II: 10-548 (JPC 3164843).

Signalment: 13-year-old, female, Thoroughbred horse (*Equus caballus*).

History: A rostral mandibular mass on the right side was noted in July 2009. Biopsy samples were non-diagnostic, showing small fragments of new bone formation with a uniform spindle cell population that may have been consistent with reactive new bone or neoplasia, though the cells were not overtly malignant. Radiographs showed an aggressive, lytic, bony lesion, and neoplasia was considered a likely differential. The horse appeared comfortable at this time. She was euthanized eight months later when the mass was perceived to be painful and she had difficulty prehending food.

Gross Pathologic Findings: The right rostral mandible is expanded by an 8 x 8 cm, well-demarcated, spherical mass with a smooth but slightly irregular surface. Cut surface of the mass is composed of firm, tan tissue with multifocal regions of cavitation (often with hemorrhage), bone lysis and mineralization. The right mandibular incisors are loose. There is a sharp demarcation between the mass and normal mandibular bone.

Laboratory Results: Cultures (aerobic and anaerobic) collected at the initial identification of the mass were negative.

Histopathologic Description: Mandibular mass: Surrounding scant remaining islands of pre-existing mandibular bone is an irregularly multilobulated, densely cellular neoplasm. Lobules are composed of sheets of cells and are separated by moderate fibrovascular stroma. The neoplastic cells are round to polygonal with indistinct cell borders and contain a scant to moderate amount of pale eosinophilic cytoplasm that surrounds a central nucleus. The nuclei are

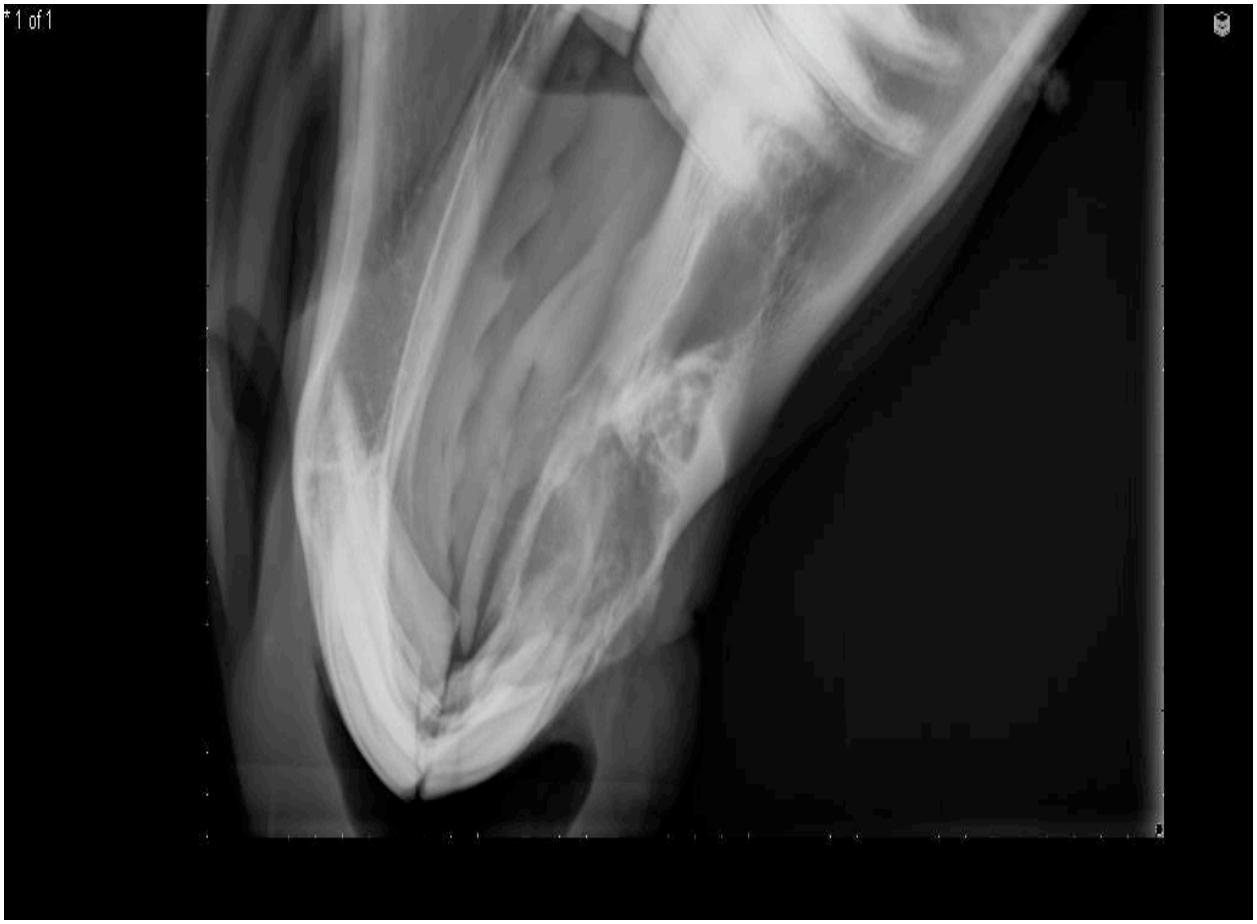

2-1. Radiograph of mandible, horse: This radiograph of a 13-year-old TB mare, taken eight months prior to autopsy, shows a lytic lesion of the right rostral mandible. (Photo courtesy of: Department of Population Health and Pathobiology, NCSU College of Veterinary Medicine, 4700 Hillsborough St. Raleigh, NC 27606. http://www.cvm.ncsu.edu)

2-2. Mandible, horse: The right rostral mandible is expanded by an 8 x 8 cm, well-demarcated, spherical mass with a smooth but slightly irregular surface. (Photo courtesy of: Department of Population Health and Pathobiology, NCSU College of Veterinary Medicine, 4700 Hillsborough St. Raleigh, NC 27606. http://www.cvm.ncsu.edu)

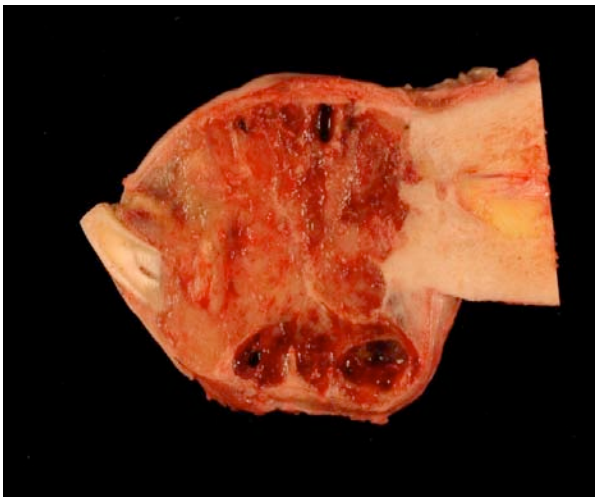

2-3. Mandible, horse: The cut surface of the mass is composed of firm, tan tissue with multifocal regions of cavitation (often with hemorrhage), bone lysis and mineralization. (Photo courtesy of: Department of Population Health and Pathobiology, NCSU College of Veterinary Medicine, 4700 Hillsborough St. Raleigh, NC 27606. http://www.cvm.ncsu.edu)

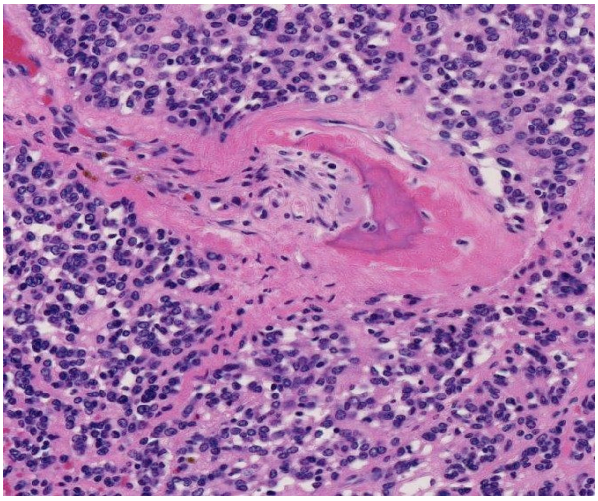

2-4. Mandible, horse: The neoplasm, which effaces mandibular bone, is composed of poorly defined streams and bundles of primitive neuroepithelium. (HE 280X)

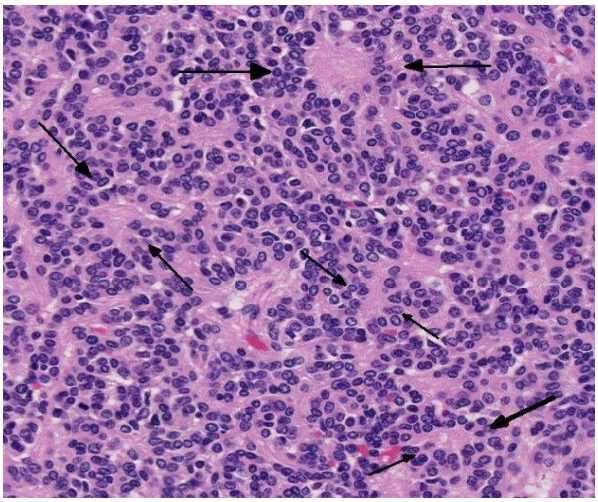

2-5. Mandible, horse: Throughout the neoplasm, neoplastic cells form rare Homer-Wright rosettes (arrows). (HE 320X)

round to oval, and sometimes reniform with coarsely clumped chromatin and rarely have 1-3 small nucleoli. Larger nuclei sometimes have a vesicular appearance to their chromatin. Within the densely cellular lobules, cells are haphazardly arranged with occasional perivascular pseudo-rosettes and rare rosettes (Homer-Wright). There is moderate anisocytosis and anisokaryosis and 6 mitotic figures per 10 high power fields are observed.

Immunohistochemically, the tumor cells show diffuse, strong staining for glial fibrillary acidic protein (GFAP), and moderate positive reactivity for vimentin and S100. About 60% of the neoplastic cells have weak to moderate cytoplasmic staining for neuron-specific enolase, and about 30% of cells have weak staining for synaptophysin.

Contributor's Morphologic Diagnosis: Peripheral primitive neuroectodermal tumor.

Contributor's Comment: Peripheral primitive neuroectodermal tumors (pPNET) are similar to the Ewing's sarcoma family of tumors (EFT). In man, there are three main types of tumors in this group including the intraosseous pPNET (Ewing's

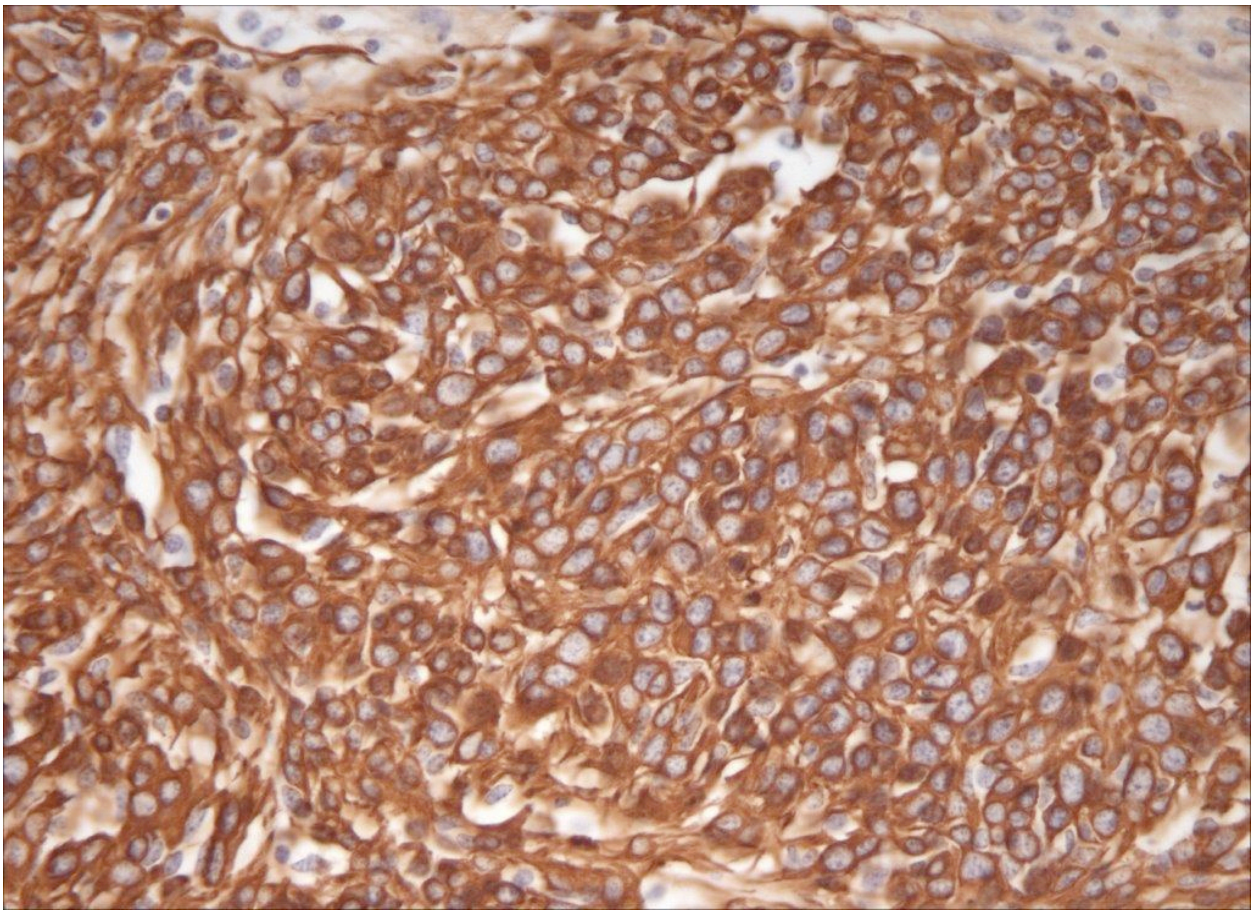

2-6. Mandible, horse: Neoplastic cells exhibit strong cytoplasmic immunoreactivity for glial fibrillary acid protein. (Photo courtesy of: Department of Population Health and Pathobiology, NCSU College of Veterinary Medicine, 4700 Hillsborough St. Raleigh, NC 27606. http://www.cvm.ncsu.edu) (anti-GFAP, 400X)

sarcoma), the extraosseous pPNET, and the thoracopulmonary Askin's tumor.[3] These tumors are rarely reported in animals, but there is a recent case reported in a camel, a few reports in dogs, and one in a Colobus monkey.[1,4,5] In people, the intraosseous tumors are most common in the long bones, but about 10% of them are reported in the skull. Of the primary tumors in the skull, approximately 10% are in the jaw bones, either the mandible or the maxilla.[3] The recently described camel pPNET had a primary vertebral mass with hepatic metastases.[5]

The pPNETs are often highly aggressive tumors composed of primitive small round cells of putative neuroectodermal phenotype, and generally occur outside the nervous system.[3,5] They often present in nests or sheets of poorly differentiated small round cells with scant cytoplasm and may have rosette or pseudorosette formation. In people, a diagnosis of EFT is strengthened with positive reactivity for MIC2 (CD99) which is not available in veterinary species, and all EFTs in people stain with neuron-specific enolase (NSE).[1,3] Variable staining for synaptophysin and S-100 has been reported in human pPNETs.

Immunohistochemistry in the few reported veterinary cases of pPNET has been somewhat inconsistent with positive triple neurofilament staining reported in one case, and variably positive or negative staining for vimentin, NSE, synaptophysin, and glial fibrillary acidic protein (GFAP).[1,4,5] The variation in reported immunohistochemistry has been postulated to be due to the variable differentiation of the neural crest progenitor cells (neuronal, ependymal, and glial).[5] Our case of a pPNET in a horse mandible most closely resembles the immunohistochemical pattern described in the recent case report in the camel with positive vimentin, GFAP, and NSE staining.

This case is also interesting because the mass was initially noted approximately eight months prior to euthanasia with no evidence of metastases at the time of necropsy, but these tumors are typically aggressive growths that often metastasize.

JPC Diagnosis: Bone, mandible: Primitive neuroectodermal tumor.

Conference Comment: As the contributor states, peripheral primitive neuroectodermal tumors (pPNET) have rarely been reported in horses; another case was recently reported in a two-year-old paint horse gelding with multiple lobulated masses bilaterally filling the scrotal cavities, extending through the inguinal canals and along the peritoneal cavity, and infiltrating both kidneys as well as the liver, spleen, mesenteric lymph nodes, mesentery and diaphragm. Histomorphological and immunohistochemical findings were consistent with a pPNET; the neoplastic cells were positive for synaptophysin, S-100, GFAP, NSE, and neurofilament protein (NFP), but negative for muscle-specific actin. Interestingly, in this gelding there appeared to be no bony involvement, whereas most pPNETs reported in veterinary literature, including the mandibular mass presented here, have significant bony involvement.[2]

Contributing Institution: North Carolina State University – College of Veterinary Medicine
Department of Population Health and Pathobiology
NCSU College of Veterinary Medicine
4700 Hillsborough St.
Raleigh, NC 27606
www.cvm.ncsu.edu

References:

1. De Cock HE, Busch MD, Fry MM, Mehl M, Bollen AW, Higgins RJ. A peripheral primitive neuroectodermal tumor with generalized bone metastases in a puppy. *Vet Pathol*. 2004;41:437-41.
2. Facemire PR, Facemire LM, Honnold SP. Peripheral primitive neuroectodermal tumor in a two-year-old paint horse. *Vet Diagn Invest.* 2012; 24:794.
3. Hadfield MG, Quezado MM, Williams RL, Luo VY. Ewing's family of tumors involving structures related to the central nervous system: a review. *Pediatr Dev Pathol*. 2000; 3:203-10.
4. Long PH, Schulman FY, Koestner A, Fix AS, Campbell MK, Cameron KN. Primitive neuroectodermal tumor in a two-month-old black and 5 white Colobus monkey. *Vet Pathol*. 1998; 35:64-7.
5. Weiss R, Walz PH. Peripheral primitive neuroectodermal tumour in a lumbar vertebra and the liver of a dromedary camel (Camelus dromedarius). *J Comp Pathol*. 2009; 141:182-6.

CASE III: V148/12 (JPC 4019895).

Signalment: A newborn, female lamb (*Ovis aries*) of unknown breed.

History: The sheep was born alive and died perinatally with a body weight of 5.3 kg. The animal originated from an area in the southeast of North Rhine-Westfalia, district of Siegen in Germany, which is approximately 50 km apart from the town of Schmallenberg.

Gross Pathology: Gross pathological findings consisted of torticollis, cerebellar hypoplasia, and hydranencephaly.

Laboratory Results: Central nervous system and blood samples were positive for Schmallenberg virus-specific genome fragments RTqPCR.

Histopathologic Description: Frontal cerebral cortex: The cerebrum shows a bilateral focally extensive reduction of the thickness of the dorsal cortex (0.5 to 1 mm) associated with cystic cavities (pores). Within the pores multiple fine strands of residual pre-existing nervous tissue are present. The affected cerebral cortex displays a severe, diffuse loss of the gray and white matter with widespread destruction of tissue architecture and accumulation of cellular debris (karyorrhectic, karyolytic and pyknotic cells) consistent with liquefactive necrosis. In addition, a low amount of irregular shaped, acellular, dark basophilic, coarsely granular material (mineralization) up to 30 µm in diameter is found scattered throughout the cortex. A moderate diffuse neuronal loss with neuronal degeneration characterized by hypereosinophilic, chromatolytic, shrunken and pyknotic neurons is found. Furthermore, few round to oval cells with a diameter up to 25 µ m, eccentric nuclei and foamy, eosinophilic cytoplasm (Gitter cells) as well as plump astrocytes containing a homogenous, eosinophilic cytoplasm (gemistocytes) are present throughout the pores. The cerebral cortex shows a diffuse and moderate capillary proliferation with prominent vessels associated with endothelial swelling (neovascularisation). Both lateral ventricles are moderately distended (up to 0.7 mm in diameter). Predominantly the gray and white matter of the ventral parts of the cerebral cortex display a moderate to severe, multifocal perivascular cuffing (up to 20 layers) and diffuse meningeal infiltration of lymphocytes and macrophages. Diffusely slight parenchymatous infiltrates are dominated by lymphocytes. In addition, rod-shaped microglial cells/macrophages (microgliosis) and astrocytes (astrogliosis) are present.

Contributor's Morphologic Diagnosis: Frontal cerebral cortex, bilateral, focally extensive

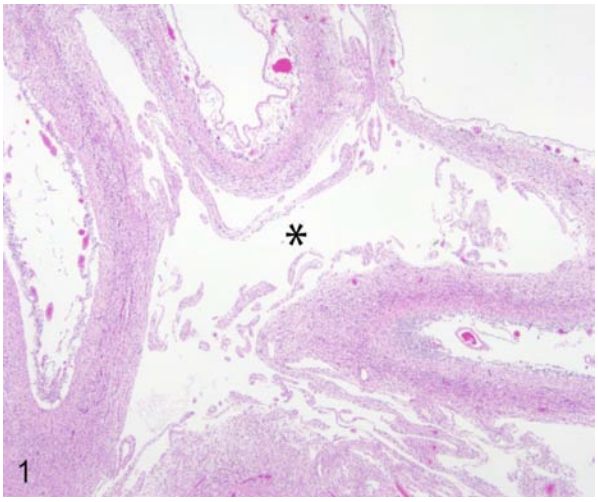

3-1. Cerebrum, lamb: Cerebral cortex of a naturally SBV-infected sheep shows widespread necrosis of the cerebral cortex with pore formation (asterisk). A thin cerebral cortex and tissue remnants of the cortex are visible as fine strands. (Photo courtesy of: Department of Pathology, University of Veterinary Medicine Hannover, Buenteweg 17, D-30559 Hannover, Germany. http://www.tiho-hannover.de/kliniken-institute/institute/institut-fuer-pathologie/) (HE)

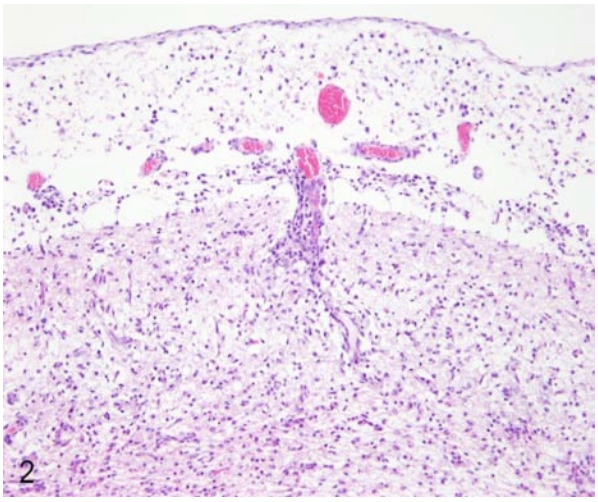

3-2. Cerebral cortex of a naturally SBV-infected sheep shows lymphohistiocytic meningoencephalitis, astro- and microgliosis and neuronal loss. (Photo courtesy of: Department of Pathology, University of Veterinary Medicine Hannover, Buenteweg 17, D-30559 Hannover, Germany. http://www.tiho-hannover.de/kliniken-institute/institute/institut-fuer-pathologie/) (HE)

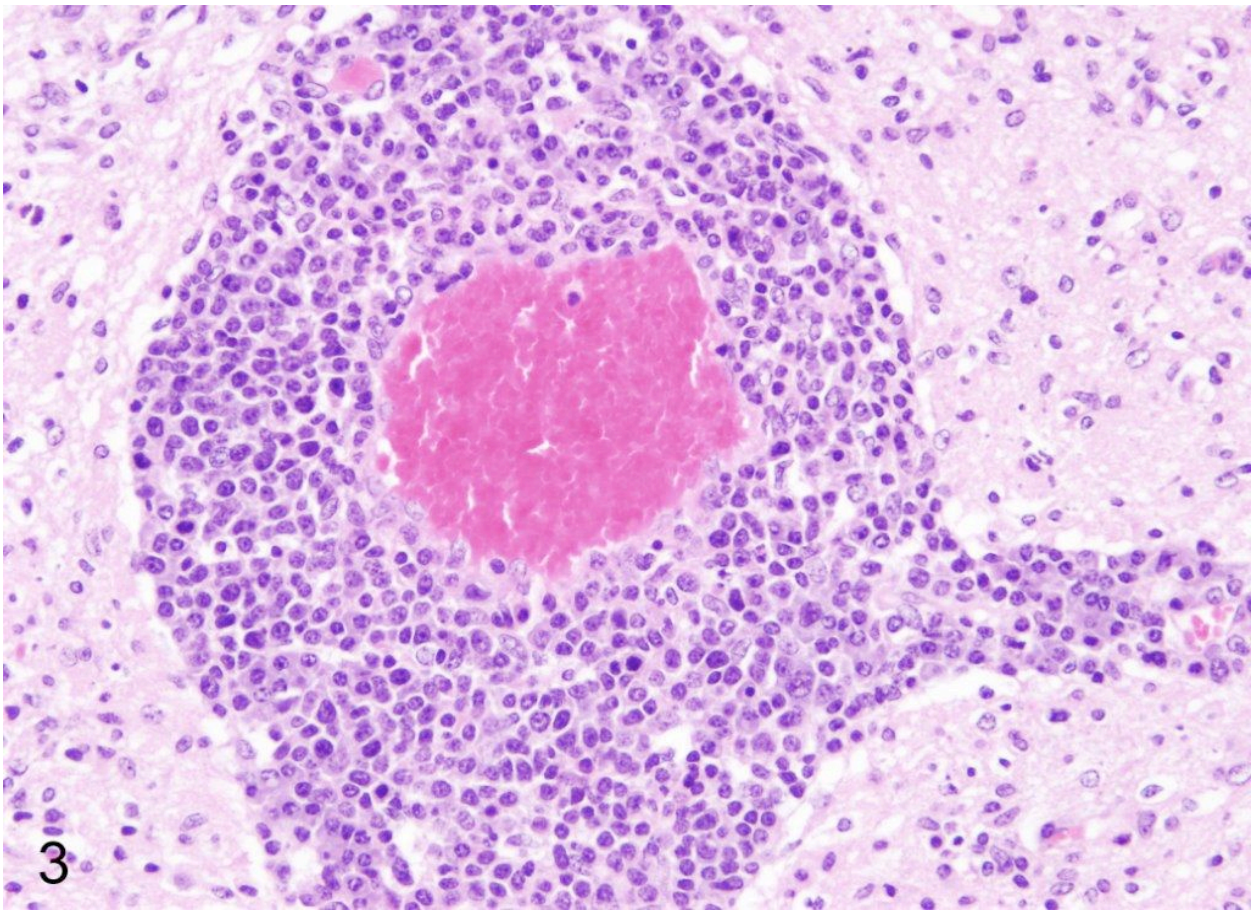

3-3. Virchow-Robin spaces contain multifocally up to 20 layers of lymphocytes and macrophages in the cerebral cortex of an SBV-infected sheep. (Photo courtesy of: Department of Pathology, University of Veterinary Medicine Hannover, Buenteweg 17, D-30559 Hannover, Germany. http://www.tiho-hannover.de/kliniken-institute/institute/institut-fuer-pathologie/) (HE)

liquefactive necrosis, severe, subacute to chronic, with cystic cavities, and meningoencephalitis, lympho-histiocytic, multifocal, subacute, moderate to severe.

Contributor's Comment: Since autumn 2011, a new emerging arthropod-borne, negative stranded ssRNA Orthobunyavirus, termed Schmallenberg virus (SBV), was detected in Europe.[11] Virus prevalence has been reported in Germany, The Netherlands, France, Belgium, Luxembourg, United Kingdom, Italy, and Spain.[7] SBV had significant economic relevance due to reduced milk yield, fever, and diarrhea in pregnant dairy cows and particularly due to abortions, and malformations of newborn ruminants.[11] Clinical signs in adult ruminants were usually limited up to a period of three weeks and affected animals recovered subsequently completely.[8] The virus was named after the town Schmallenberg in western Germany, because the first identification of the virus succeeded in samples of cattle housed next to this town. Similar to other Orthobunyaviruses, like Akabane virus, SBV causes malformations in newborn ruminants due to a prenatal infection. Macroscopically, malformations comprise arthrogryposis, vertebral malformations, brachygnathia inferior as well as various central nervous system (CNS) malformations like hydranencephaly, porencephaly, internal hydrocephalus, cerebellar hypoplasia and micromyelia in lambs, goat kids and calves.[10] Until now, it is not known how exactly SBV arrived in Germany, but parallels were made to the epidemiology of Blue tongue virus, which emerged first in Europe in 2006 and is also transmitted via arthropods.[17] Possible routes of SBV entry to Europe are insects and/or animals in aircrafts or import of cut flowers from Africa.[17]

Based on metagenomic analysis,[11] SBV belongs to a group of teratogenic viruses causing arthrogryposis and hydranencephaly (AG/HE).

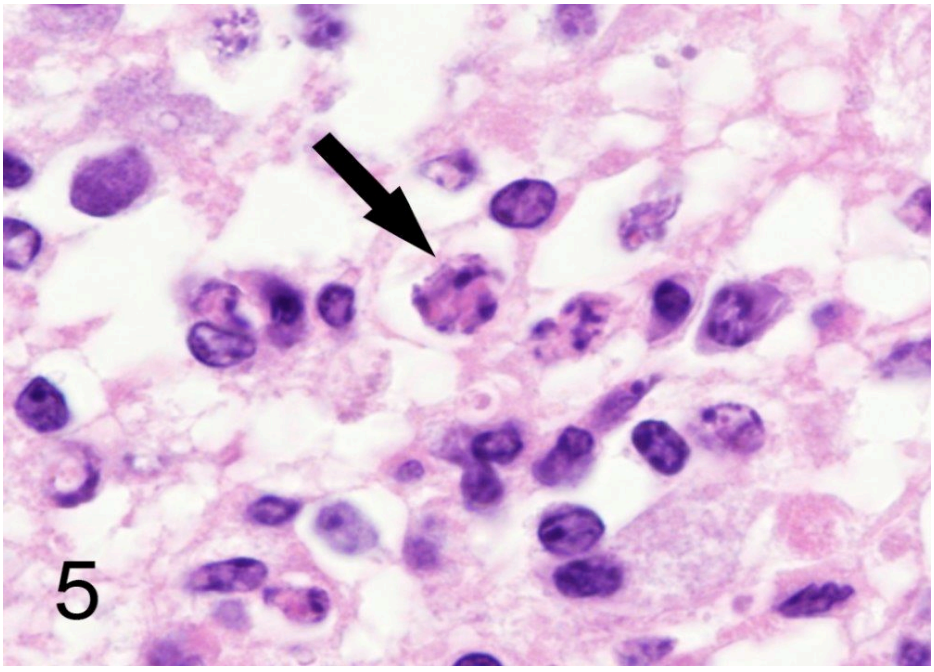

3-4. Thin cortical areas of a SBV-infected sheep contain necrotic neurons with karyorrhexis and karyolysis (arrow). (Photo courtesy of: Department of Pathology, University of Veterinary Medicine Hannover, Buenteweg 17, D-30559 Hannover, Germany. http://www.tiho-hannover.de/kliniken-institute/institute/institut-fuer-pathologie/) (HE)

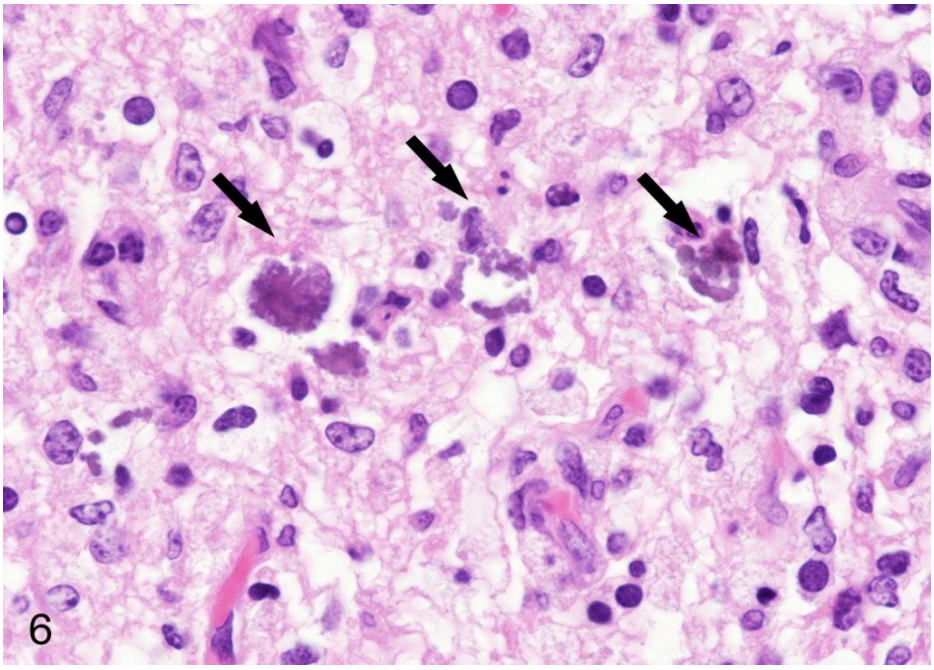

3-5. Cortical liquefactive necrosis of a SBV-infected sheep displays multifocal deposition of basophilic, coarse granular, extracellular material (arrows). (Photo courtesy of: Department of Pathology, University of Veterinary Medicine Hannover, Buenteweg 17, D-30559 Hannover, Germany. http://www.tiho-hannover.de/kliniken-institute/institute/institut-fuer-pathologie/) (HE)

These malformations in cattle caused by Akabane virus represent an entity called "*enzootic bovine arthrogryposis and hydranencephaly*".[20]

Until now the pathogenesis of SBV infection is not fully understood. Due to a genetic relationship to other viruses of the genus *Orthobunyavirus*, a similar pathogenesis is suggested.[1,2] Furthermore, the SBV-induced pathology cannot be differentiated from infections with Akabane virus[12] which requires an identification at the molecular level with PCR.[11] Appropriate samples for the detection of viral nucleotides by means of this technique are external placental fluid, umbilical cord, cerebrum, and spinal cord.[2] Placental fluid and umbilical cord samples can be taken easily without necropsy. The central nervous system is accessible in animals submitted for necropsy without placental fluid and only umbilical cord remnants.[2] Spleen, cartilage, placental fluid from the stomach, and meconium rarely revealed a positive PCR result in SBV-infected animals and therefore these samples should be avoided for virus detection.[2] In addition, placenta and placental fluid of SBV-infected animals contain huge amounts of virus.[2] So far the host range of SBV seems to be restricted to ruminants and there is no evidence of a zoonotic risk.[6]

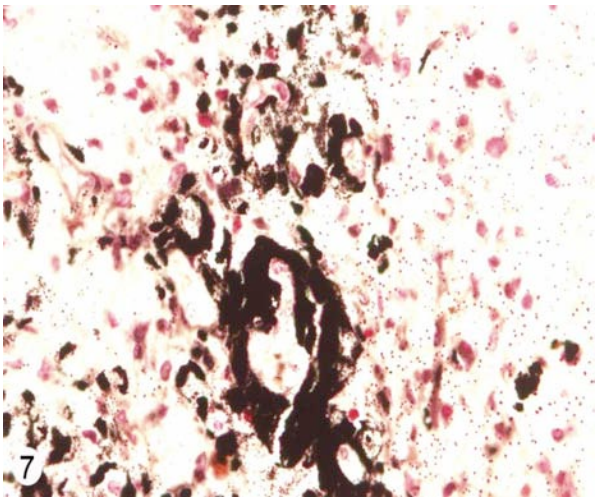

3-6. Remaining cortical tissue of a SBV-infected sheep displays multifocally moderate to severe mineralizations, which stained black with von Kossa's stain. (Photo courtesy of: Department of Pathology, University of Veterinary Medicine Hannover, Buenteweg 17, D-30539 Hannover, Germany. http://www.tiho-hannover.de/kliniken-institute/institute/institut-fuer-pathologie/) (Von Kossa)

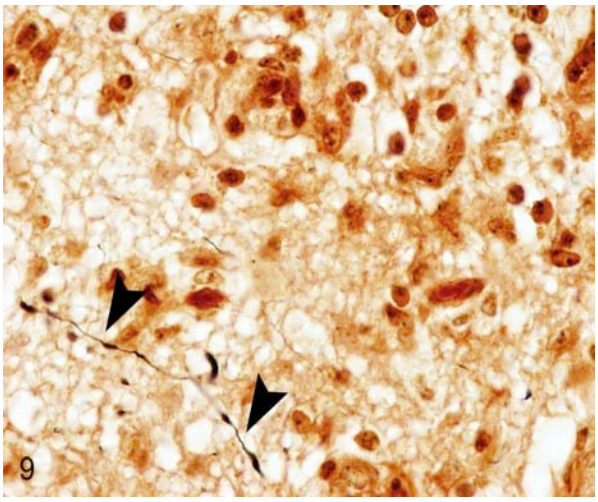

3-7. The cerebral cortex of an SBV-infected sheep displays reduced axonal density in areas with necrosis, inflammation and mineralization. Only few remaining silver impregnated axons are visible (arrowheads). (Photo courtesy of: Department of Pathology, University of Veterinary Medicine Hannover, Buenteweg 17, D-30559 Hannover, Germany. http://www.tiho-hannover.de/kliniken-institute/institute/institut-fuer-pathologie/) (Bielchowsky silver impregation)

A recent study compared genomic RNA of SBV with Sathuperi and Shamonda viruses indicating that all viruses belong the genus *Orthobunyavirus* and that SBV originates from a re-assortment of Sathuperi and Shamonda virus.[26]

In general, climate change is suggested to be the most important factor for the occurrence of arthropod-borne virus-infections in Europe.[9] SBV is supposed to be transmitted by arthropods, but the high numbers of initial SBV infections in Europe suggest additional routes of transmission, e.g. direct contact, fecal-oral route or aerosols.[1]

Interestingly, in the present case the lambs' CNS showed liquefactive necrosis with porencephaly and additional non-suppurative inflammation. Studies with the closely related Akabane virus showed that the virus crosses the placenta after viremia and replicates in fetal cells of the central nervous system. The virus prefers rapidly dividing cells and causes damage to neurons.[24] Depending on the time point of infection, CNS pathology varies. According to Akabane virus infection, it is suggested that transplacental SBV infection at early stages of gestation causes severe brain lesions, like hydranencephaly due to a widespread loss of neuronal tissue. The severity of brain damage is less extensive, if the infection occurs to a later time point of gestation. Infection during the 2nd trimester may result in a more focal necrosis of the CNS characterized by porencephaly. This porencephaly can be associated with a meningoencephalitis.[20] Assuming that Akabane virus and SBV have a similar pathogenesis, an infection during the 2nd trimester is suggested in the present case. Our study revealed that only 20% (12 out of 58 animals) of all RTqPCR positive tested CNS samples of ruminants (lambs, goat kids and calves) showed meningoencephalitis with or without CNS malformations.[10] Infiltration of lymphocytes and macrophages showed a perivascular pattern. Furthermore, gitter cell formation and neuronal necrosis were present. For further characterization of the lesions several special stains were applied including von Kossa´s stain, Luxol fast-blue stain, and Bielschowsky´s silver impregnation. Intralesional amorphous basophilic material stained positive with a von Kossa stain indicating intralesional mineralization, which was found multifocally in the thin cortical areas of the pore. Demyelination was shown as reduced staining intensity in the cortex containing pores. Bielschowsky´s silver impregnation was used to investigate the extent of axonal alterations. The amount of positive axons was reduced.

The included table lists possible etiological differentials of SBV infection. The described histopathological lesions are not characteristic for a particular virus. The etiology has to be proven with other methods, e.g. molecular techniques,

like PCR. Further epidemiological information as well as the geographical area (e.g. Asia, Europe, USA) of occurrence have to be considered. The table summarizes information of naturally infected animals; results of experimentally infected animals were not included.

Table 1: Overview on virus infections, their pathology in offspring after natural transmission, susceptible species and the transmission mode representing possible etiological differentials of Schmallenberg virus infection.

Virus	Disease name	Gross findings	Histology	Species	Transmission
Schmallenberg virus[4,10,11] Orthobunyavirus, Bunyaviridae		Arthrogryposis, vertebral malformations, brachygnathia inferior, hydran- and porencephaly, internal hydrocephalus, cerebellar hypoplasia, micromyelia	Lymphohistiocytic meningoencephalomyelitis, CNS malacia, gliosis, muscular hypoplasia	Ruminants: sheep, goats, cattle, bisons	Arbovirus: mosquitos and midges: e. g. *Culex obsoletus*, *Culex dewulfi*
Akabane virus[3,13,15,16,18,22] Orthobunyavirus, Bunyaviridae	Enzootic bovine arthrogryposis and hydranencephaly; congenital arthrogryposis-hydranencephaly syndrome (CAHS)	Arthrogryposis, vertebral malformations, hydranencephaly, CNS cyst formation	Non-suppurative encephalomyelitis, neuronal loss in the spinal cord, muscular dysplasia	Herbivores: cattle, horses, donkeys, sheep, goats, camels, buffaloes, pigs	Arbovirus: mosquitos and midges, eg. *Culex sp., Aedes sp., Culicoides imicola*
Bovine virus diarrhea virus[20] Pestivirus, Flaviviridae		Cerebellar hypoplasia, mummification, runting, microencephaly, hydranencephaly, hydrocephalus, microphthalmia, cataract, brachygnathism, thymic aplasia, hypotrichosis, alopecia, pulmonary hypoplasia	perivascular non-suppurative meningeal infiltration, CNS malacia, hypomyelinogenesis, retinal degeneration, optic neuritis, myocarditis,	Cattle, sheep, goat, pig,	Excretions, inhalation, ingestion, semen, contaminated embryo transfer fluid
Blue tongue virus[19,20] Orbivirus, Reoviridae		Porencephaly, hydranencephaly, hydrocephalus, subcortical cysts, cerebellar dysgenesis, runting	Necrotizing meningoencephalitis, interstitial pneumonia, mononuclear cells in kidney and liver	Sheep, wild ruminants, camelids, cattle, zoo carnivores[14]	Arbovirus: *Culicoides sp.*
Border disease virus[20] Pestivirus, Flaviviridae	Border disease Condition: "hairy shaker"	Embryonic death, mummification, fleece abnomalities, runting, cerebellar hypo- and dysplasia, micro-, por- and hydranencephaly, leukoencephalomalacia, micro-myelia, starvation, cardiac abnormalities, rarely: arthrogryposis, kyphoscoliosis	Dys- and hypomyelination	Sheep, goats, pigs, cattle	Oral, conjuctival, intranasal, genital, semen
Cache valley virus, syn. Bunyamwera virus[5,20] Orthobunyavirus, Bunyaviridae		Arthrogryposis, hydrocephalus, hydranencaphaly, microcephaly, vertebral malformations, cerebellar hypoplasia, micromelia, porencephaly	Necrosis and loss of neuropil and motor neurons, myositis, poorly developed myocytes	Sheep, deer, caribou, pigs, horses, cattle, raccoons, foxes, man	Arbovirus: *Culicoides sp., Culiseta sp., Anopheles sp.*
Chuzan virus, **syn. Palyamvirus**[20] Orbivirus, Reoviridae		Hydranencephaly, cerebellar hypoplasia, hydrocephalus, microcephaly		Cattle	Arbovirus: *Culicoides oxystoma*
Classical swine fever virus[20] Pestivirus, Flaviviridae	Hog cholera	Mummification, runting, stillbirth, pulmonary hypoplasia, pulmonary artery malformation, micrognathia, arthrogryposis, cerebellar hypoplasia, microcephaly, defective myelination	Necrotizing vasculitis in CNS, intestine, skin, lymphoid depletion, endothelial degeneration, valvular fibrosis, portal fibrosis (liver), interstitial pneumonia, neuronal degeneration	Pigs, cattle, sheep, goats	Excretions, ingestion
Rift valley fever virus[20,23] Phlebovirus, Bunyaviridae		Intra-uterine fetal death	Hepatic necrosis, acidophilic intranuclear inclusions, cholestasis, degeneration of lympho-cytes, heart muscle and renal tubules	Sheep, cattle, goats, man	Arbovirus: *Aedes sp., Culex sp.*
Wesselsbron virus[20] Flavivirus, Flaviviridae		Mummification, hydranencephaly, arthrogryposis, hydrops amnii, porencephaly, cerebellar hypoplasia	Non-suppurative meningoencephalomyelitis, eosinophilic, intranuclear inclusions, liver: degeneration, necrosis, Kupffer cell hyperplasia, hepatitis, hyper- and inflammation of bile ducts	Sheep, cattle, man	Arbovirus
Aino virus, syn. Shuni virus[3,21,25] Orthobunyavirus, Bunyaviridae	Arthrogryposis-hydranencephaly syndrome (CAHS)	Hydranencephaly, arthrogryposis, cerebellar hypoplasia	Necrotizing encephalopathy, perivascular cuffing with lymphoid cells, neuronal mineralization	Cattle, sheep	Arbovirus: *Culicoides brevitarsis, Culex tritaeniorhynchus*

JPC Diagnosis: Brain, cerebrum: Necrosis, liquefactive, bilateral, focally extensive, with marked gliosis, mineralization, spheroid formation, lymphohistiocytic meningoencephalitis and hydrocephalus ex vacuo.

Conference Comment: The contributor provides an excellent and thorough description of this emerging Orthobunyavirus. Conference participants commented on the presence of band-like areas of microvascular proliferation (increased vascular pattern) present in the section, and speculated that these were likely due to collapse of the parenchyma, vessel dilation, and a compensatory induction of new vessel formation secondary to the release of cytokines and factors [i.e. vascular endothelial growth factor (VEGF)] associated with the inflammatory response and hypoxic conditions within these areas of parenchymal collapse.

Contributing Institution: Department of Pathology
University of Veterinary Medicine Hannover
Buenteweg 17
D-30559 Hannover
Germany
http://www.tiho-hannover.de/kliniken-institute/institute/institut-fuer-pathologie/

References:

1. Scenarios for the future spread of Schmallenberg virus. *Veterinary Record.* 2012;170:245-246.
2. Bilk S, Schulze C, Fischer M, Beer M, Hlinak A, Hoffmann B. Organ distribution of Schmallenberg virus RNA in malformed newborns. *Veterinary Microbiology*. 2012:159:236-8.
3. Brenner J, Tsuda T, Yadin H, Chai D, Stram Y, Kato T. Serological and clinical evidence of a teratogenic Simbu serogroup virus infection of cattle in Israel, 2001-2003. *Vet Ital.* 2004;40:119-123.
4. Conraths F, Beer M, Peters M. "Schmallenberg-Virus": Eine neue Infektionskrankheit bei Wiederkäuern. *Tierärztliche Umschau.* 2012;5:147-150.
5. Edwards JF, Livingston CW, Chung SI, Collisson EC. Ovine arthrogryposis and central nervous system malformations associated with in utero Cache Valley virus infection: spontaneous disease. *Veterinary Pathology.* 1989;26:33-39.
6. Eurosurveillance editorial team: European Food Safety Authority publishes its second report on the Schmallenberg virus. *Euro Surveillance.* 2012;17: pii=20140.
7. Garigliany MM, Hoffmann B, Dive M, Sartelet A, Bayrou C, Cassart D, et al. Schmallenberg virus in calf born at term with porencephaly, belgium. *Emerging Infectious Diseases*. 2012;18:1005-1006.
8. Gibbens N. Schmallenberg virus: a novel viral disease in northern Europe. *Vet Rec.* 2012;170:58.
9. Gould EA, Higgs S, Buckley A, Gritsun TS. Potential arbovirus emergence and implications for the United Kingdom. *Emerging Infectious Diseases.* 2006;12:549-555.
10. Herder V, Wohlsein P, Peters M, Hansmann F, Baumgärtner W. Salient lesions in domestic ruminants infected with the emerging so-called Schmallenberg Virus in Germany. *Veterinary Pathology*. 2012;49(4):588-91.
11. Hoffmann B, Scheuch M, Höper D, Jungblut R, Holsteg M, Schirrmeier H, et al. Novel orthobunyavirus in cattle, Europe, 2011. *Emerging Infectious Diseases.* 2012;18:469-472.
12. Höper D, Wernike K, Eschbaumer M, Conraths F, Hoffmann B, Schirrmeier H, et al. "Schmallenberg-Virus" - Ein neues Virus in Europa. *Deutsches Tierärzteblatt*. 2012;4:500-505.
13. Huang CC, Huang TS, Deng MC, Jong MH, Lin SY. Natural infections of pigs with akabane virus. *Veterinary Microbiology.* 2003;94:1-11.
14. Jauniaux TP, De Clercq KE, Cassart DE, Kennedy S, Vandenbussche FE, Vandemeulebroucke EL, et al. Bluetongue in Eurasian lynx. *Emerging Infectious Diseases.* 2008;14:1496-1498.
15. Konno S, Moriwaki M, Nakagawa M. Akabane disease in cattle: congenital abnormalities caused by viral infection. Spontaneous disease. *Veterinary Pathology.* 1982;19:246-266.
16. Kono R, Hirata M, Kaji M, Goto Y, Ikeda S, Yanase T, et al. Bovine epizootic encephalomyelitis caused by Akabane virus in southern Japan. *BMC Vet Res.* 2008;4:20.
17. Kupferschmidt K. Infectious disease. Scientists rush to find clues on new animal virus. *Science.* 2012;335:1028-1029.
18. Lee JK, Park JS, Choi JH, Park BK, Lee BC, Hwang WS, et al. Encephalomyelitis associated with akabane virus infection in adult cows. *Veterinary Pathology.* 2002;39:269-273.

19. Maclachlan NJ, Drew CP, Darpel KE, Worwa G. The pathology and pathogenesis of bluetongue. *Journal of Comparative Pathology*. 2009;141:1-16.
20. Maxie M, Youssef S. Jubb, Kennedy, and Palmer's Pathology of Domestic Animals. 5th ed. Vol. 1-3. Philadelphia, PA: Saunders Elsevier; 2007.
21. Noda Y, Uchinuno Y, Shirakawa H, Nagasue S, Nagano N, Ohe R, et al. Aino virus antigen in brain lesions of a naturally aborted bovine fetus. *Veterinary Pathology.* 1998;35:409-411.
22. Parsonson IM, McPhee DA, Della-Porta AJ, McClure S, McCullagh P. Transmission of Akabane virus from the ewe to the early fetus (32 to 53 days). *Journal of Comparative Pathology.* 1988;99:215-227.
23. Rippy MK, Topper MJ, Mebus CA, Morrill JC. Rift Valley fever virus-induced encephalomyelitis and hepatitis in calves. *Veterinary Pathology.* 1992;29:495-502.
24. St. George T, Kirkland P. Diseases caused by Akabane and related Simbu-group viruses. In: Coetzer J, Tustin R, eds. Infectious Diseases of Livestock. 2nd edition. eds. 2nd ed. Oxford, UK: Oxford University Press; 2004:1029-1036.
25. Uchinuno Y, Noda Y, Ishibashi K, Nagasue S, Shirakawa H, Nagano M, et al. Isolation of Aino virus from an aborted bovine fetus. *Journal of Veterinary Medical Science.* 1998;60:1139-1140.
26. Yanase T, Kato T, Aizawa M, Shuto Y, Shirafuji H, Yamakawa MT. Genetic reassortment between Sathuperi and Shamonda viruses of the genus Orthobunyavirus in nature: implications for their genetic relationship to Schmallenberg virus. *Archives of Virology*, 2012;157(8):1611-6.

CASE IV: E884/12 (JPC 4019397).

Signalment: 9-year-old, spayed female, Basset hound, dog, (*Canis lupus familiaris)*.

History: The dog had generalized seizures, intermittent tremor, high amplitude myoclonia and altered behavior since a few weeks. The seizures were controlled with antiepileptic drugs over a period of 4 weeks prior to euthanasia.

Gross Pathology: Only the formalin fixed brain of the animal was obtained and no gross lesions were noted.

Histopathologic Description: Brain, cerebral cortex: Multifocally and haphazardly distributed within the white and gray matter, nerve cell bodies, axons, dendrites and occasional the neuropil contain large, up to 20 µm in diameter, round, basophilic to amphophilic inclusions. Nerve cell bodies are enlarged up to 40 µm in diameter by the inclusions and most nuclei are compressed or displaced to the periphery. Inclusions have a homogeneous core with a more faintly staining radiating periphery and are PAS-positive, also accentuating their structure. Multifocally neurons contain fine granular golden-brown pigment in their cytosol (lipofuscin). Additionally, there is mild, multifocal satellitosis and mild diffuse increase in microglia.

Contributor's Morphologic Diagnosis: Brain, cerebral cortex: Polyglucosan (Lafora) bodies, diffuse, numerous with mild multifocal satellitosis and microgliosis.

Contributor's Comment: Lafora disease (LD) is a rare autosomal recessive disorder that was first described in humans in 1911 by a Spanish neurologist named Gonzalo Rodríguez Lafora. Clinically, this neurologic disorder is characterized by early onset during adolescence

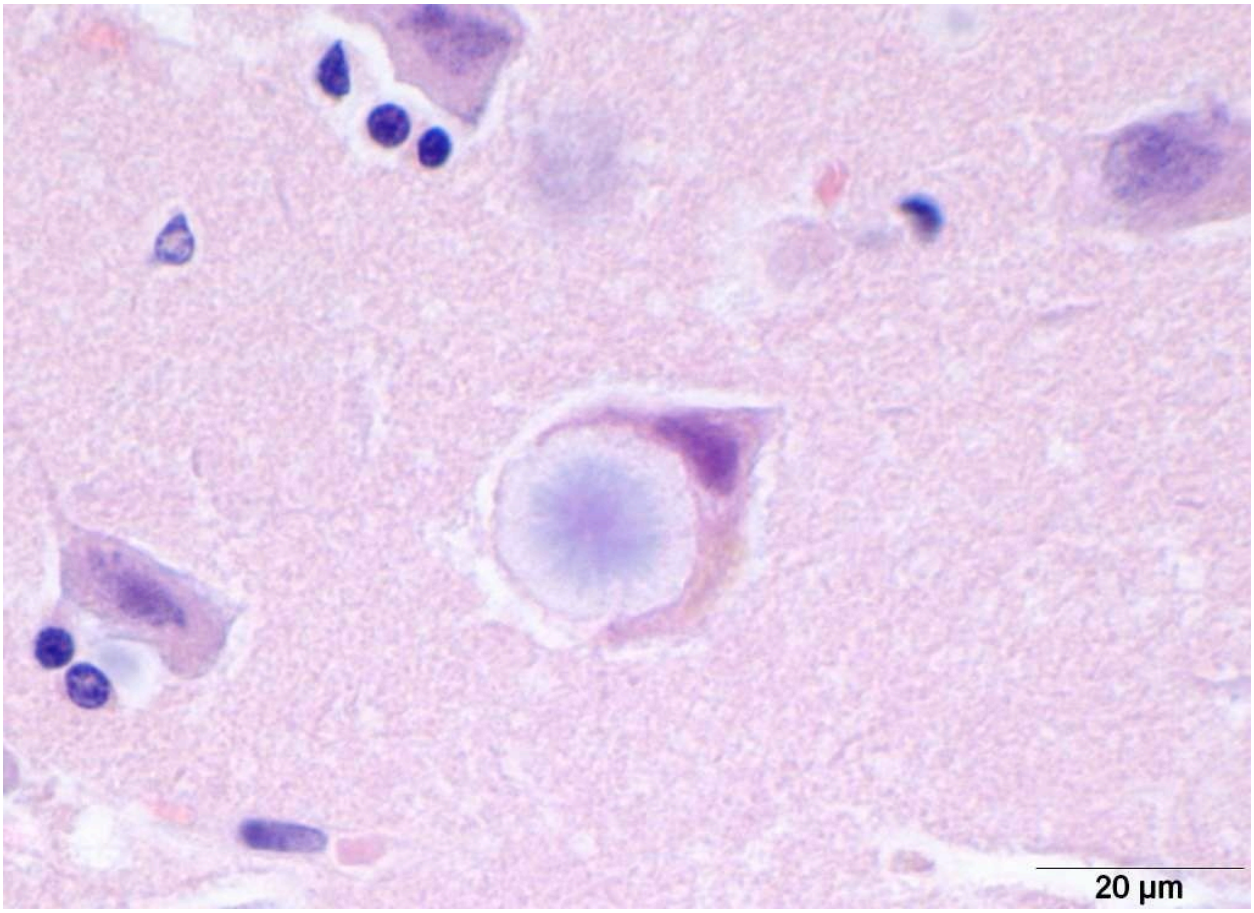

4-1. Cerebral cortex, dog: Within the white and gray matter, nerve cell bodies, axons, and dendrites contain large, basophilic to amphophilic inclusions ranging up to 20 µm in diameter. (Photo courtesy of: Institute of Veterinary Pathology, Freie Universitat Berlin, Robert-von-Ostertag-Straße 15, Building 12 14163 Berlin, Germany, http://www.vetmed.fu-berlin.de/en/einrichtungen/institute/we12) (HE)

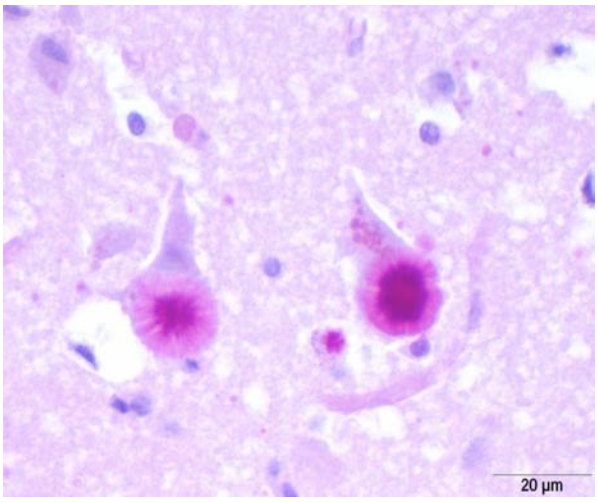

4-2. Cerebral cortex, dog: Inclusions have a homogeneous core with a more faintly staining radiating periphery (Fig. 1) and are PAS-positive, also accentuating their structure. (Photo courtesy of: Institute of Veterinary Pathology, Freie Universitat Berlin, Robert-von-Ostertag-Straße 15, Building 12 14163 Berlin, Germany, http://www.vetmed.fu-berlin.de/en/einrichtungen/institute/we12) (Periodic acid-Schiff)

of symptoms including stimulus-sensitive grand mal tonic-clonic, absence, visual and myoclonic seizures. The disease then rapidly progresses to dementia, psychosis, cerebellar ataxia, dysarthria, amaurosis, mutism, muscle wasting and respiratory failure leading to death within 10 years after onset.[2,12,17] It is most commonly seen in populations and parts of the world where there is a high rate of consanguinity.[4]

Histopathologically, LD is characterized by the presence of pathognomonic inclusions named Lafora bodies (LB) especially in the brain, spinal cord and other tissues such as skin, liver, cardiac and skeletal muscle.[2] In the central nervous system LB are localized mostly in the perikarya. These inclusions can become very large, leading to cell death.[1]

LB are carbohydrate storage products that are composed of polyglucosans, which are abnormally formed glycogen molecules that resemble starch. This polyglucosans are poorly branched which makes them insoluble leading to the formation of the characteristic intracellular inclusions.[14]

In most cases this disorder is caused by mutations in one of two different genes, EPM2A and EPM2B (also known as NHLRC1) which encode the proteins laforin and malin, respectively.[3,11] Laforin is a glycogen phosphatase which plays an important role in glycogen metabolism and is involved in dephosphorylation of complex carbohydrates such as amylopectin and glycogen and thus preventing the soluble glycogen molecules from becoming insoluble polyglucosans.[9] Malin on the other hand is an E3 ubiquitin ligase that is believed to target laforin catalyzing its polyubiquitination and thus its degradation. However, the specific role of malin in this process is yet to be

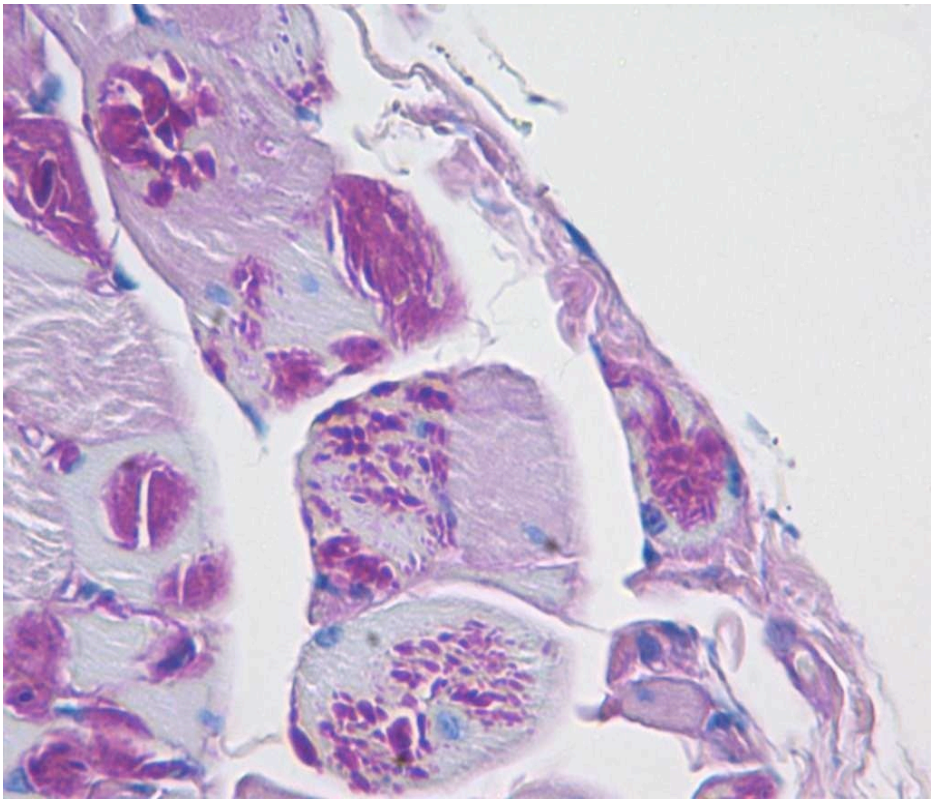

4-3. Cranial tibial muscle, dog: Microsciopic examination revealed istopathological analysis and accumulations of PAS-positive, diastase-resistant, brightly staining material forming focal intraparenchymal subsarcolemmal accumulations consistent with Lafora bodies were found in the skeletal muscle fibers. (Photo courtesy of: Institute of Veterinary Pathology, Freie Universitat Berlin, Robert-von-Ostertag-Straße 15, Building 12, 14163 Berlin, Germany, http://www.vetmed.fu-berlin.de/en/einrichtungen/institute/we12) (Periodic acid-Schiff)

determined.[9]

In the dog LD has been reported in the Basset Hound, Miniature Wirehaired Dachshund, Poodle and Beagle also.[8,18] In these animals progressive myoclonus is associated with the presence of intraneuronal storage of complex polyglucosans forming the so-called LB.[8]

LB in the dog appear as spherical basophilic to amphophilic, mostly intracytoplasmatic inclusions with peripheral radiating filaments; their size may vary from 5 to 20 µm and can be localized in the dendrites, axons or perikarya (unlike in humans).[2] LB may be found anywhere along the neuroaxis and retinal ganglion cells but in dogs with neuronal disease they are most common in the Purkinje cells and neurons of the caudate, thalamic and periventricular nuclei.[18] LB are PAS positive, diastase resistant, stain positively with Best's carmine, methenamine silver, and Weil's.[7] In electron microscopy, they are not membrane bound and are composed of fibrillary and electron-dense, sometimes granular components in varying proportions. They are often associated with rough endoplasmic reticulum and Golgi. LB present as accumulations of insoluble complex glycoprotein polymers that need to be distinguished from other types of polyglucosan bodies such as Lafora-like bodies, corpora amylacea, and amylopectin bodies.[14] The distinction between LB and other inclusions is performed based on clinical features and tissue distribution of the inclusions.[15]

Corpora amylacea are inclusions that are formed in normal aging cells and are chemically and histochemically indistinguishable from LB. Corpora amylacea can be found in axons and astrocytic processes but not in the perikarya, unlike LB.[15]

Amylopectin bodies are formed in patients with glycogen storage disease type IV or glycogen branching enzyme deficiency.[19,20] They result from accumulation of abnormal polysaccharides and are mostly indistinguishable from LB in terms of morphology and distribution and thus the clinical presentation of the disease should be used in their distinction.[19,20]

Lafora-like bodies are also very similar in their morphology and distribution but are observed in normal aged animals without neurologic symptoms.[19]

In cases of LD, typically LB are also found in skeletal muscle samples where they lie between myofibrils or beneath the sarcolemma and therefore muscle biopsies can be used for the diagnosis of the disease.[15] In the case presented here, a biopsy of the cranial tibial muscle was submitted for histopathological analysis and accumulations of PAS positive, diastase resistant, brightly staining material forming focal intraparenchymal subsarcolemmal accumulations consistent with LB were found in the skeletal muscle fibers.

The canine counterpart of LD seems to be associated with a mutation in the *EPM2B* gene, more precisely a dodecamer expansion in the gene.[10] This mutation was observed in 5% of Miniature Wirehaired Dachshunds in England.[10]

The presence of LB associated with neurologic disease has also been documented in cats and cows.[5,16] A recent report described a Lafora´s-like disease in a fennec fox (*Vulpes zerda*)[7] and another report demonstrated LB in the brain of an aged captive raccoon (*Procyon lotor*).[6]

JPC Diagnosis: Brain, cerebrum, frontal lobes: Polyglucosan bodies, intraneuronal, numerous.

Conference Comment: As the contributor states in this informative summary of Lafora's disease, the genetic mutation in dogs involves the *EPM2B* gene. Recently a DNA test for the autosomal recessive mutation that identifies "clear," "carrier," and "affected" dogs has been developed and is currently available in the United Kingdom.[13]

Contributing Institution: Department of Veterinary Pathology
Freie Universität Berlin, Germany
http://www.vetmed.fu-berlin.de/en/einrichtungen/institute/we12/index.html

References:

1. Andrade DM, Ackerley CA, Minett TS, et al. Skin biopsy in Lafora disease: genotype-phenotype correlations and diagnostic pitfalls. *Neurology.* 2003;61:1611-1614.
2. Andrade DM, Turnbull J, Minassian BA. Lafora disease, seizures and sugars. *Acta* Myol. 2007;26:83-86.

3. Chan EM, Young EJ, Ianzano L, et al. Mutations in NHLRC1 cause progressive myoclonus epilepsy. *Nat Genet.* 2003;35:125-127.
4. Delgado-Escueta AV, Ganesh S, Yamakawa K. Advances in the genetics of progressive myoclonus epilepsy. *Am J Med Genet*. 2001;106:129-138.
5. Hall DG, Steffens WL, Lassiter L. Lafora bodies associated with neurologic signs in a cat. *Veterinary Pathology.* 1998;35:218-220.
6. Hamir AN. Spontaneous lesions in aged captive raccoons (Procyon lotor). *J Am Assoc Lab Anim Sci.* 2011;50:322-325.
7. Honnold SP, Schulman FY, Bauman K, et al. Lafora's-Like Disease in a Fennec Fox (Vulpes Zerda). *J Zoo Wildlife Med.* 2010;41:530-534.
8. Jubb KVF, Kennedy PC, Palmer NC. *Pathology of Domestic Animals*. 5th ed. Philadelphia, PA: Saunders Elsevier; 2007;898.
9. Knecht E, Aguado C, Sarkar S, et al. Impaired autophagy in Lafora disease. *Autophagy.* 2010;6:991-993.
10. Lohi H, Young EJ, Fitzmaurice SN, et al. Expanded repeat in canine epilepsy. *Science.* 2005;307:81-81.
11. Minassian BA, Ianzano L, Delgado-Escueta AV, et al. Identification of new and common mutations in the EPM2A gene in Lafora disease. *Neurology.* 2000;54:488-490.
12. Minassian BA. Lafora's disease: towards a clinical, pathologic, and molecular synthesis. *Pediatr Neurol.* 2001;25:21-29.
13. Sainsbury R. DNA scrrening for Lafora's disease in miniature wire-haired dachshunds. *Vet Rec*. 2011;169:292.
14. Sakai M, Austin J, Witmer F, et al. Studies in myoclonus epilepsy (Lafora body form). II. Polyglucosans in the systemic deposits of myoclonus epilepsy and in corpora amylacea. *Neurology.* 1970;20:160-176.
15. Schoeman T, Williams J, van Wilpe E. Polyglucosan storage disease in a dog resembling Lafora's disease. *J Vet Intern Med*. 2002;16:201-207.
16. Simmons MM. Lafora Disease in the Cow. *Journal of Comparative Pathology* 1994;110:389-401.
17. Singh S, Ganesh S. Lafora progressive myoclonus epilepsy: a meta-analysis of reported mutations in the first decade following the discovery of the EPM2A and NHLRC1 genes. *Hum Mutat.* 2009;30:715-723.
18. Summers BA, Cummings JF, de Lahunta A. *Veterinary Neuropathology*. 1st ed. St. Louis, MO: Mosby: 1995:527.
19. Suzuki Y, Akiyama K, Suu S. Lafora-like inclusion bodies in the CNS of aged dogs. *Acta Neuropathol*. 1978;44:217-222.
20. Suzuki Y, Ohta K, Kamiya S, et al. Topographic distribution pattern of Lafora-like bodies in the spinal cord of some animals. *Acta Neuropathol.* 1980;49:159-161.